New Phase Boundary in Highly Correlated, Barely Metallic V_2O_3

S. A. Carter,[1] T. F. Rosenbaum,[2] J. M. Honig,[3] and J. Spalek[4]
[1]*The James Franck Institute and Department of Chemistry, The University of Chicago, Chicago, Illinois 60637*
[2]*The James Franck Institute and Department of Physics, The University of Chicago, Chicago, Illinois 60637*
[3]*Department of Chemistry, Purdue University, West Lafayette, Indiana 47907*
[4]*Department of Physics, Purdue University, West Lafayette, Indiana 47907*
(Received 12 September 1991)

We compare the magnetic and transport properties of the low-temperature metal in nonstoichiometric and compressed vanadium sesquioxide. Antiferromagnetic order is robust for the full range of vanadium vacancy concentrations, but it can be suppressed with modest hydrostatic pressures. The temperature-pressure phase diagram for V_2O_3 thus includes a new $T=0$ boundary between antiferromagnetic and paramagnetic metals. Furthermore, analysis of the $T\rightarrow 0$ diffusive metallic conductivity at the approach to the insulator-metal transition indicates a different role for correlations depending upon the means employed to effect the transition.

PACS numbers: 71.30.+h, 72.15.−v, 75.30.Kz

Vanadium sesquioxide has served as the prototype for both the Mott-Hubbard model of the metal-insulator transition [1,2] and the Brinkman-Rice picture [3–5] of the correlated metal. Pure V_2O_3 undergoes a first-order metal-insulator (MI) transition at a temperature $T_{MI}\sim 150$ K with drastic changes in the electrical resistivity and antiferromagnetic ordering of the vanadium spins, and a structural transition. The application of hydrostatic pressure, the adjustment of the oxygen stoichiometry, and alloying with titanium sesquioxide serve to depress T_{MI}, and, in sufficient degree, can stabilize the metallic phase at all temperatures [6,7]. This variation of the T_{MI} with internal (chemical) and/or external pressure gives rise to a generalized phase diagram [8,9] for V_2O_3 which has provided the framework for some of the original studies of highly correlated insulators and metals.

More recently, it was found that the metallic phase also undergoes an antiferromagnetic transition at low temperature [10,11], with $T_N\sim 10$ K. In this paper, we demonstrate that antiferromagnetic ordering in the metal can be suppressed completely. In so doing, we show that changing the oxygen stoichiometry and applying hydrostatic pressure give rise to very different magnetic phase diagrams for metallic V_2O_3. Finally, we use the diffusive nature of the transport in the $T\rightarrow 0$ limit to probe the role of the electron-electron interactions as the insulator-metal transition is approached from above. We find that the role of correlations depends on the process by which the metallic phase is stabilized.

Single crystals of V_2O_3 were grown using a skull melter [12]. Thin plates were then annealed in a suitable CO-CO_2 atmosphere at 1400 °C for approximately 2 weeks to adjust the stoichiometry uniformly [13]. Four-probe resistivity measurements on oriented samples of typical dimensions $1\times 1\times 3$ mm^3 were made using a standard lock-in technique at 16 Hz for $0.02\ \text{K}\leq T\leq 300$ K. All results were obtained in the Ohmic and frequency-independent regimes. Pressures up to 7 kbar were achieved using a BeCu hydrostatic pressure cell which was designed to fit into the top-loading chamber of a dilution refrigerator. We used silicone oil as the pressure medium and a small piece of $(V_{0.99}Ti_{0.01})_2O_3$ for pressure calibration; its T_{MI} changed by 5.8 K/kbar [8,14]. Magnetic susceptibility measurements were made in a commercial SQUID magnetometer for $1.8\ \text{K}\leq T\leq 300$ K.

The antiferromagnetic transition in the metal is marked by a classic hard-axis–easy-axis response in the susceptibility [15]. We plot in Fig. 1 the ac magnetic susceptibility parallel to the $\hat{\mathbf{a}}$ axis for a series of metallic $V_{(2-y)}O_3$ crystals. Increasing the number of vanadium vacancies pushes the system toward the more metallic state, with a critical concentration for the $T=0$ metal-insulator transition of $V_{1.985}O_3\equiv V_2O_{3.023}$. We show in the inset to Fig. 1 the magnetic susceptibilities of the five metals to higher temperature. All the curves deviate considerably from Curie-Weiss behavior below $T\approx 50$ K, with an increasing enhancement in the peak magnitude of

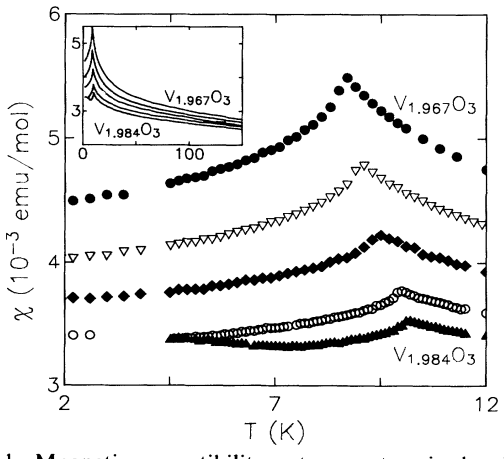

FIG. 1. Magnetic susceptibility vs temperature in the vicinity of the antiferromagnetic transition in the metal. $V_{(2-y)}O_3$ stoichiometries vary from just above the insulator-metal transition to well into the metal, but T_N changes only slightly. Data are shown for vacancy concentrations $y=0.016$, 0.018, 0.021, 0.026, and 0.033. Inset: Overview of the magnetic transition.

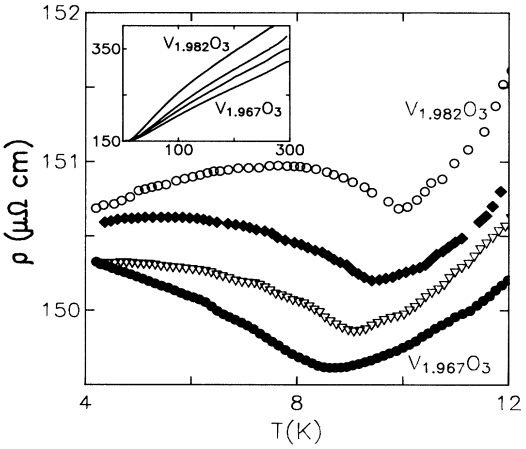

FIG. 2. Resistive temperature minimum accompanies the peak in the magnetic susceptibility at the metallic antiferromagnetic transition. Data are shown for $y=0.018$, 0.021, 0.026, and 0.033. Inset: Overview of the temperature dependence of the electrical resistivity.

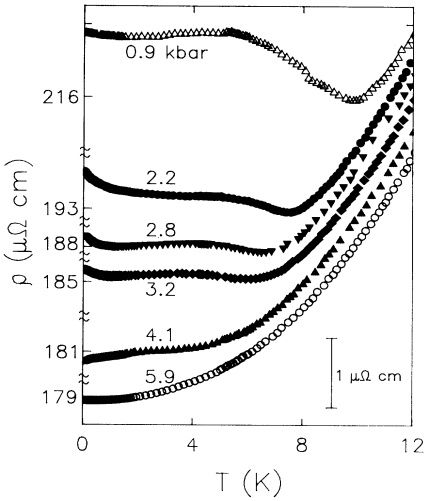

FIG. 3. Resistivity data corresponding to Fig. 2, but here as a function of hydrostatic pressure for a $V_{1.986}O_3$ crystal. The minimum, denoting T_N, moves quickly to lower T with increasing P. Metallic antiferromagnetism is completely suppressed by $P=6$ kbar.

χ with increasing y. By contrast, the Néel temperature changes very little with vanadium vacancy concentration. The small decrease of T_N with increasing y requires the blown-up temperature scale of the main part of the figure to be discerned.

The cusp in the magnetic susceptibility is accompanied by a minimum in the electrical resistivity. As shown in Fig. 2, the resistivity minimum tracks the slight movement of T_N with changes in the sample stoichiometry. The occurrence of a minimum at the antiferromagnetic phase transition has been explained in terms of wave-vector-dependent critical scattering of electrons by spin fluctuations [16], and has been observed in a host of other antiferromagnetic metals (e.g., dysprosium [17], Cr:Mo alloys [18], and higher-order members of the Magneli series [19], V_nO_{2n-1}).

We provide in the inset of Fig. 2 a global perspective on $\rho(T)$ for the oriented metallic crystals. At highest temperatures, the resistivity is effectively linear in T. At lower temperature, there is a crossover in ρ to a superlinear temperature dependence, which is cut off at low T by the minimum associated with the antiferromagnetic ordering of the spins. In the temperature range 10 to 25 K, the resistivity approaches the form $\rho \propto T^2$, indicative of a large electron-electron scattering term within the Brinkman-Rice [3] framework for a strongly correlated metal [20]. At the lowest temperatures ($T<1$ K), $\rho \propto T^{1/2}$, a form characteristic of electron-electron interactions in the presence of disorder, as discussed in detail below.

We show in Fig. 3 the metallic resistivity data analogous to Fig. 2, but this time for a series of hydrostatic pressures. The measurements were made on a single crystal of $V_{1.986}O_3$, which at $P=0$ is just insulating ($T_{MI} \approx 35$ K), and requires a pressure $P \sim 0.5$ kbar to become metallic at all T. Here we see again the minimum in $\rho(T)$ marking the opening of the antiferromagnetic gap. Now, however, the resistivity minimum moves rapidly down in temperature as the metal is traversed with increasing pressure. For $P \sim 6$ kbar, $T_N \rightarrow 0$ and the low-temperature metal is no longer magnetic.

The data of Figs. 1–3 indicate that it is no longer appropriate to map nonstoichiometric and compressed V_2O_3 onto the same generalized phase diagram. We contrast in Fig. 4 the phase diagrams as functions of y and P, where the latter now includes the additional boundary at $T=0$ between antiferromagnetic metal and paramagnetic metal. We have set the relative scales of the abscissas using the relationship $y/P=0.015/(20$ kbar), derived from appropriate measurements on the insulator [6–9,14]. As one check on this relationship, we have repeated our pressure experiments from deeper within the insulator and find that a crystal with $T_{MI} \approx 70$ K maps onto the bottom half of Fig. 4 with the expected pressure offset ~ 2 kbar.

The discovery of a new phase boundary in the canonical Mott-Hubbard system raises a number of questions: (1) Why has it not been seen before? One reason is apparent from the phase diagram itself: the narrow slice in pressure and the low temperatures required to access the antiferromagnetic metal. (2) Why is the antiferromagnetic order stable against both changes in the oxygen stoichiometry [10] and Ti substitution [11], but not against hydrostatic pressure? Neutron-scattering studies would be most helpful in answering this question, but it is not unreasonable to expect that wave-function overlap forced by pressure could more profoundly alter nesting

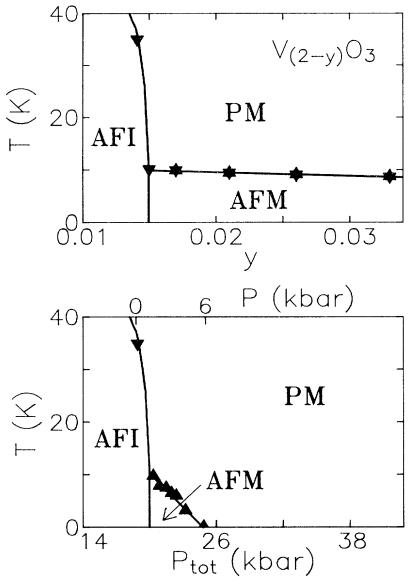

FIG. 4. Contrasting phase diagrams for vanadium vacancy concentration y and hydrostatic pressure P. P_{tot} is the sum of the internal chemical pressure and the applied pressure P, using the stoichiometry-pressure correspondence established in the insulator (Refs. [6–9,14]). AFI denotes antiferromagnetic insulator; AFM, antiferromagnetic metal; and PM, paramagnetic metal. Up (down) triangles are from resistivity (susceptibility) data.

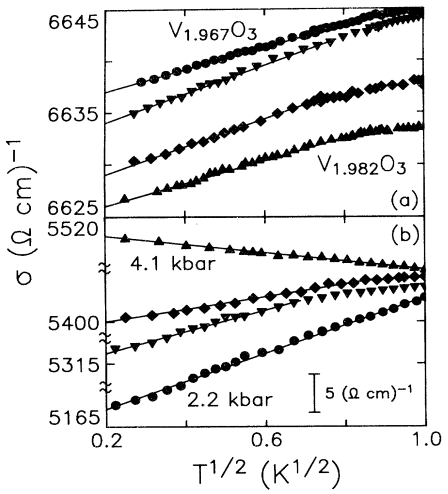

FIG. 5. Square-root temperature dependence of the conductivity characteristic of electron-electron interactions in the presence of disorder. (a) Nature of the metallic diffusive transport appears essentially independent of vanadium vacancy concentration, y=0.018, 0.021, 0.026, and 0.033. (b) Slope of the $T^{1/2}$ term (proportional to carrier effective mass) markedly depends on pressure, P=2.2, 2.8, 3.2, and 4.1 kbar, with a concomitantly faster change in $\sigma(0)$ at the approach to the metal-insulator transition.

conditions on the Fermi surface than either the introduction of vacancies or on-site disorder. (3) Is the new low-temperature paramagnet in the high-pressure regime of Fig. 4 the true ground state? A superconducting transition might occur in metallic V_2O_3 in light of its close proximity to a Mott-Hubbard insulator (cf. rare-earth oxide superconductors) and the important role of correlations (cf. heavy-fermion superconductors). We find no evidence of superconductivity on either side of the antiferromagnetic-paramagnetic boundary for $T \geq 0.02$ K. It may be, however, that our nonstoichiometric samples are sufficiently disordered to preclude superconductivity even at low T [21]. (4) Given that the $T \rightarrow 0$ phase diagram for the metal is different for V vacancies and pressure, one should raise the question of whether the $T \rightarrow 0$ insulator-metal transition also differs for the two cases.

In order to help answer the last question, we have compared the $T \rightarrow 0$ charge transport for the two cases as the insulator-metal transition is approached from above. We plot in Figs. 5(a) and 5(b) the conductivity σ vs $T^{1/2}$ for a series of stoichiometries and pressures, respectively. The $T^{1/2}$ dependence is characteristic of electron-electron interactions in the presence of disorder in the diffusive metal [22]. In such a case, $\sigma(T)=\sigma(0)+\alpha(\frac{4}{3}-2F)T^{1/2}$, where $\alpha=[T_F(m^*D/\hbar)]^{-1/2}$, T_F is the Fermi temperature, m^* is the effective mass, and D is the diffusion constant for charge carriers subject to random walks. The dimensionless term F is a function of the Fermi and screening wave vectors ranging from 0 to 1, thereby permitting the $T^{1/2}$ correction to $\sigma(0)$ to be either positive or negative.

The slope of the $T^{1/2}$ term remains essentially unchanged as a function of oxygen stoichiometry [Fig. 5(a)], even to within 0.3% of the transition in y. A simple effective-mass enhancement from electron correlations should show up as a change in slope. We note that heat-capacity measurements [23] on these same samples do lead to a large Sommerfeld constant γ, but, in accord with the transport data, show little change at the approach to the metal-insulator transition. $\gamma(T \rightarrow 0)$, which is proportional to m^*, actually decreases from 145 mJ/mol K for $V_{1.967}O_3$ to 118 mJ/mol K for $V_{1.984}O_3$, following the behavior of T_N.

In marked contrast to the results of adjusting the stoichiometry, the diffusive conductivity prefactor changes rapidly with hydrostatic pressure in the antiferromagnetic metal, with a concomitantly faster change in $\sigma(0)$ [Fig. 5(b)]. The $T^{1/2}$ slope is metalliclike at the paramagnetic-metal–antiferromagnetic-metal boundary, switches sign as the antiferromagnetic order develops, and becomes more and more insulating as the metal-insulator transition nears. The larger negative slope at lower P is consistent with a simple effective-mass enhancement from correlations. Alternatively, the electron-electron interactions in the presence of disorder could be modified by the magnetic order, perhaps through changes in the diffusion constant D or in the screening process.

Our results show for the first time that there are profound differences in the properties of the low-temperature metallic phase of nonstoichiometric and compressed vanadium sesquioxide. Hydrostatic pressure can completely suppress antiferromagnetic order, introducing an additional $T=0$ phase boundary between antiferromagnetic metal and paramagnetic metal. Moreover, characterization of the $T \rightarrow 0$ diffusive conductivity indicates that electron interaction effects enter differently into the physics of the metal-insulator transition in the two cases. In Anderson transitions, dominated by disorder, contrasts in the diffusive metallic transport reflect different critical exponents at the transition. For Si:P [24], the $T^{1/2}$ slope changes rapidly near the metal-insulator transition (like compressed V_2O_3), and the critical exponent for $\sigma(0)$ is $\nu=\frac{1}{2}$. For amorphous Nb:Si [25], the $T^{1/2}$ slope is constant at the approach to the transition (like nonstoichiometric V_2O_3) and $\nu=1$. A determination of whether there are different universality classes at the $T=0$ Mott-Hubbard transition awaits a more complete characterization of the present mix of charge, spin, lattice, and localization effects.

We have benefited greatly from conversations with E. Abrahams and R. Bhatt. We are grateful to P. Metcalf for annealing the V_2O_3 crystals used in this research. T.F.R. thanks the Aspen Center for Physics where some of this work was accomplished. The work at The University of Chicago was supported by Grant No. NSF DMR 8816817. J.M.H. and J.S. were supported by MISCON Grant No. DE-FG02-90ER45427.

[1] D. B. McWhan, T. M. Rice, and J. P. Remeika, Phys. Rev. Lett. **23**, 1384 (1969).
[2] N. F. Mott, Proc. Phys. Soc. London A **62**, 416 (1949); J. Hubbard, Proc. R. Soc. London A **281**, 401 (1964).
[3] W. F. Brinkman and T. M. Rice, Phys. Rev. B **2**, 4302 (1970).
[4] D. B. McWhan *et al.*, Phys. Rev. Lett. **27**, 941 (1971).
[5] J. Spalek, M. Kokowski, and J. M. Honig, Phys. Rev. B **39**, 4175 (1989).
[6] N. F. Mott, *Metal-Insulator Transitions* (Taylor and Francis, London, 1974), Chap. 5, and references therein.
[7] S. A. Shivashankar and J. M. Honig, Phys. Rev. B **28**, 5695 (1983), and references therein; J. Spalek, A. Datta, and J. M. Honig, Phys. Rev. Lett. **59**, 728 (1987).
[8] D. B. McWhan *et al.*, Phys. Rev. B **7**, 1920 (1973).
[9] H. Kuwamoto, J. M. Honig, and J. Spalek, Phys. Rev. B **22**, 2626 (1980).
[10] Y. Ueda, K. Kosuge, and S. Kachi, J. Solid State Chem. **31**, 171 (1980).
[11] J. Dumas and C. Schlenker, J. Magn. Magn. Mater. **7**, 252 (1978).
[12] J. E. Keem *et al.*, Am. Ceram. Soc. Bull. **56**, 1022 (1977); H. R. Harrison, R. Aragon, and C. J. Sandberg, Mater. Res. Bull. **15**, 571 (1980).
[13] S. A. Shivashankar *et al.*, J. Electrochem. Soc. **128**, 2472 (1981); **129**, 1641(E) (1982).
[14] S. A. Carter *et al.*, Phys. Rev. B **43**, 607 (1991).
[15] T. F. Rosenbaum and S. A. Carter, J. Solid State Chem. **88**, 94 (1990).
[16] S. Alexander, J. S. Helman, and I. Balberg, Phys. Rev. B **13**, 304 (1976); Y. Suezaki and H. Mori, Prog. Theor. Phys. **41**, 1177 (1969).
[17] R. A. Craven and R. D. Parks, Phys. Rev. Lett. **31**, 383 (1973).
[18] G. T. Meaden, K. V. Rao, and K. T. Lee, Phys. Rev. Lett. **25**, 359 (1970).
[19] P. C. Canfield, J. D. Thompson, and G. Gruner, Phys. Rev. B **41**, 4850 (1990).
[20] For $\rho=\rho_0+AT^2$ and $10 \leq T \leq 25$ K, we find $A=0.055$ $\mu\Omega$ cm/K^2 for $V_{1.986}O_3$ under pressure. This compares well with the value $A=0.054$ $\mu\Omega$ cm/K^2 for $T \leq 25$ K reported by McWhan *et al.* (Ref. [8]) for V_2O_3 under pressure.
[21] G. T. Zimanyi and E. Abrahams, Phys. Rev. Lett. **64**, 2719 (1990).
[22] B. L. Altshuler, A. G. Aronov, and P. A. Lee, Phys. Rev. Lett. **44**, 1288 (1980); T. F. Rosenbaum *et al.*, Phys. Rev. Lett. **46**, 568 (1981). For a review, see P. A. Lee and T. V. Ramakrishnan, Rev. Mod. Phys. **57**, 287 (1985).
[23] S. A. Carter *et al.* (to be published).
[24] T. F. Rosenbaum *et al.*, Phys. Rev. B **27**, 7509 (1983).
[25] G. Hertel *et al.*, Phys. Rev. Lett. **50**, 743 (1983).